

NASA Technical Memorandum 102322

# Total Hemispherical Emittance Measured at High Temperatures by the Calorimetric Method

(NASA-TN-102322) TOTAL HEMISPHERICAL  
EMITTANCE MEASURED AT HIGH TEMPERATURES BY  
THE CALORIMETRIC METHOD (NASA) 1989  
USCIB 138

100-10007

03/91 0752615

Frank DiFilippo  
*Case Western Reserve University*  
*Cleveland, Ohio*

Michael J. Mirtich and Bruce A. Banks  
*Lewis Research Center*  
*Cleveland, Ohio*

Curtis Stidham and Michael Kussmaul  
*Cleveland State University*  
*Cleveland, Ohio*

Prepared for the  
16th International Conference on Metallurgical Coatings  
sponsored by the American Vacuum Society  
San Diego, California, April 17-21, 1989

**NASA**



# TOTAL HEMISPHERICAL EMITTANCE MEASURED AT HIGH TEMPERATURES

## BY THE CALORIMETRIC METHOD

Frank DiFilippo\*  
Case Western Reserve University  
Cleveland, Ohio 44106

Michael J. Mirtich and Bruce A. Banks  
National Aeronautics and Space Administration  
Lewis Research Center  
Cleveland, Ohio 44135

Curtis Stidham and Michael Kussmaul  
Cleveland State University  
Cleveland, Ohio 44115

### ABSTRACT

A calorimetric vacuum emissometer (CVE) capable of measuring total hemispherical emittance of surfaces at elevated temperatures was designed, built, and tested. Several materials with a wide range of emittances were measured in the CVE between 773 to 923 K. These results were compared to values calculated from spectral emittance curves measured in a room temperature Hohlraum reflectometer and in an open-air elevated temperature emissometer. The results differed by as much as 0.2 for some materials but were in closer agreement for the more highly-emitting, diffuse-reflecting samples. The differences were attributed to temperature, atmospheric, and directional effects, and errors in the Hohlraum and emissometer measurements ( $\pm 5$  percent). The probable error of the CVE measurements was typically less than 1 percent.

### INTRODUCTION

Some proposed space power systems (solar dynamic and nuclear, for example) will require large radiators for waste heat rejection. The mass and size of the radiators will be minimized by using a material with a high thermal emittance. The goal for the SP-100 system radiators (fig. 1) is a total emittance of 0.85 or better at an operating temperature of 700 to 900 K.

Many methods, such as sandblasting (ref. 1), ion-beam discharge chamber texturing (ref. 2), and carbon arc electrical discharge texturing (ref. 3), have been used at NASA Lewis Research Center to achieve high emittance. Spectral emittance measurements between 1.7 and 14.7  $\mu\text{m}$  have been made at room temperature using the Hohlraum reflectivity attachment of a Perkin-Elmer Model 13 spectrophotometer and at elevated temperature (900 K) using the emissivity attachment (ref. 4). The total emittance was then calculated by normalizing the spectral emittance to the blackbody radiation distribution function at the desired temperature.

---

\*Summer Intern at NASA Lewis Research Center.

Although these methods have been used by many experimenters to calculate total emittance (ref. 5), the values obtained may not be equal to the total hemispherical emittance at elevated temperature. The spectral emittance of materials can be temperature dependent. For example, the Hagen-Rubens relation states that the spectral emissivity of metals is proportional to the resistivity to the one-half power for wavelengths longer than about 5  $\mu\text{m}$  (ref. 6). Hence, the spectral emittance of pure metals can be expected to increase with temperature, along with the resistivity. Other factors which affect the spectral emittance are surface chemistry and morphology, which often change as a result of heating to 900 K in a reactive atmosphere such as air (ref. 4). Additionally, there may be problems with directional effects. The Hohlraum attachment measures hemispheric-angular spectral reflectance, and the emissivity attachment measures normal spectral emittance, neither of which measures total hemispherical emittance.

An instrument which actually measured total hemispherical emittance without being subject to the above complications was the calorimetric vacuum emissometer (CVE). By conducting high temperature measurements under vacuum with the sample surface radiating hemispherically, the effects of temperature, surface chemistry, and directionality were minimized, yielding results more comparable to those expected in space. Total emittance measurements for materials with a wide range of emittances were measured using the CVE, the Hohlraum reflectometer, and the emissometer. The measured total emittance values are presented and compared along with an evaluation of the relative uncertainties.

## APPARATUS AND PROCEDURE

The CVE used in this experiment originally had been designed to measure total emittance of 5.1 by 5.1 cm (2 in. by 2 in.) samples at 323 to 423 K by means of a heat flux transducer (ref. 7). The sample holder and heater needed to be redesigned in order to make measurements at temperatures between 700 to 900 K, but the remaining components of the instrument were unchanged. The vacuum chamber and pump system for the CVE are shown in figure 2. The system consisted of a mechanical pump and diffusion pump which enabled pressures of about  $5 \times 10^{-5}$  torr to be reached in about 2 hr. A cylindrical blackbody cavity cooled with liquid nitrogen was supported inside the vacuum chamber. Two type T thermocouples were used to monitor the temperature of cavity and the liquid nitrogen exit port. The base pressure was typically  $5 \times 10^{-7}$  torr when the cavity was cooled with liquid nitrogen. The interior of the cavity was coated with 3M Nextel Black Velvet paint, which has an emissivity of about 0.95. The emissivity of the cavity (40 cm long, 15 cm diameter) was calculated to be about 0.998 by the method of Gouffé (ref. 8).

A photograph of the redesigned sample holder for the CVE is shown in figure 3. A cutaway drawing of the sample heater/holder is shown in figure 4. There were two main components of the sample heater/holder: the heat shield and the sample mount plate. The heat shield was a 8.26 cm (3.25 in.) long, 4.45 cm (1.75 in.) diameter copper cylinder with swaged nichrome heater wire (1.0 mm (0.040 in.) diameter) coiled around and brazed to the cylinder. Copper wire leads connected the heater wire to a Kepco 36 V, 8 A dc power supply. Two 1.0 mm (0.040 in.) diameter swaged type K thermocouples were peened into the heat shield to measure the temperature at both the front and back. The

sample mount plate (fig. 5) was a hollowed copper disk, 22.2 mm (0.875 in.) in diameter and 6.4 mm (0.250 in.) thick. A 1.0 mm (0.040 in.) diameter swaged type K thermocouple was peened in the center of the sample mount plate, and a 1.0 mm (0.040 in.) diameter swaged nichrome heater wire was brazed to the inside of the plate. The nichrome wire was terminated inside the sample mount plate, and 0.5 mm (0.020 in.) diameter copper wire leads were attached to the nichrome wire with 0.5 mm (0.020 in.) diameter copper connectors. The copper leads were insulated with ceramic beads and were coiled inside the heat shield to improve thermal contact. A Kepco 25 V, 20 A dc power supply was used for heating the sample mount plate. The back side of the sample mount plate was covered with three 0.25 mm (0.010 in.) thick tantalum disks, which served as radiation shielding. The entire sample holder assembly was mounted to the flange of the vacuum chamber by means of two 6.4 mm (0.25 in.) diameter stainless steel rods. The flange also contained several feedthroughs to which the heater leads and thermocouple leads were connected.

The sample holder was designed for samples which could also be used in the Hohlräum reflectivity attachment and the emissivity attachment of a Perkin-Elmer Model 13 spectrophotometer. The samples were 2.38 (15/16 in.) to 2.54 cm (1 in.) diameter disks with thicknesses ranging from 0.4 mm (0.015 in.) to 1.9 mm (0.075 in.). The sample temperature was measured with a 0.25 mm (0.010 in.) diameter swaged type K thermocouple which was peened to the back side of the sample through a milled groove (fig. 6). Carbon paint was used to bind the sample to the sample mount plate to improve thermal contact. Before mounting, the back side of the sample and the front side of the sample mount plate were coated lightly with GC Electronics Television Tube Koat carbon paint and allowed to dry. Afterwards, more carbon paint was applied to the sample mount plate, and the sample was placed on top of the plate and held in place for about 1 min until the paint was dry enough to hold the sample. The thermocouple lead was wrapped around the heat shield twice before it was connected to the flange. The sides and front of the heat shield were covered with two sheets of tantalum foil radiation shielding to reduce the power needed for heating. A tantalum foil ring was placed around the sample and sample mount plate; the ring was made wide enough so that the sides of the sample could not be seen, preventing radiation from the sample edge. The sample and sample mount plate were held lightly in place with four 0.5 mm (0.020 in.) diameter stainless steel prongs. Figure 7 shows a photograph of a properly mounted sample.

After high vacuum ( $<10^{-4}$  torr) was reached, the heat shield and sample mount plate were heated to the desired temperature, and the cavity was cooled to liquid nitrogen temperature. The power supplies were adjusted until the heat shield and sample mount plate remained at the desired temperature for about 8 min. Afterwards, the sample mount plate heater current, the sample temperature, and the cavity temperature were recorded. Data were taken for sample mount plate temperatures of 923, 873, 823, and 773 K.

It was also important to know accurately the electrical resistance of the sample mount plate heater. For this measurement, copper voltage leads with ceramic bead insulation were spot welded to the sample mount plate heater connectors. The sample mount plate and heat shield were heated in vacuum to 923, 873, 823, and 773 K, and the measured voltage and current were used to calculate the resistance at these temperatures. The voltage leads were removed when samples were run to reduce heat conduction losses.

## THEORY

A schematic of the experiment is shown in figure 8. The heated sample was allowed to radiate hemispherically to the cavity so that an equilibrium temperature was established. The current and resistance for the sample mount plate heater were measured, and the total power input to the sample could then be calculated. The experiment was designed to virtually eliminate all other forms of power dissipation besides radiation to the cavity. Much of this goal was accomplished by using the heat shield, which was maintained at the same temperature as the sample mount plate. Afterwards, the total hemispherical emittance could be calculated from the Stefan-Boltzmann radiation law.

Figure 9 illustrates the possible sources of heat generation and dissipation from the sample and sample mount plate. Mathematically, the heat flows can be expressed by the following heat balance equation:

$$Q_{e1} + Q_{abs} = Q_{rad} + Q_{cond} + mC_p \left( \frac{dT}{dt} \right) \quad (1)$$

where

- $Q_{e1}$             power introduced by the sample mount plate heater
- $Q_{abs}$            power gained by the absorption of radiation
- $Q_{rad}$            power lost by radiation
- $Q_{cond}$           power lost through thermal conduction
- $mC_p(dT/dt)$    power causing a temperature change in the sample and sample mount plate ( $m$  = mass,  $C_p$  = heat capacity,  $T$  = temperature,  $t$  = time)

The  $Q_{rad}$  and  $Q_{cond}$  terms on the right side of the equation (1) each consist of several individual terms. Power could be radiated by the front surface of the sample to the cavity ( $Q_{rad,f}$ ), by the sides of the sample and the sample mount plate ( $Q_{rad,s}$ ), and by the back side of the sample mount plate ( $Q_{rad,b}$ ):

$$Q_{rad} = Q_{rad,f} + Q_{rad,s} + Q_{rad,b} \quad (2)$$

During the experiment, the sample mount plate and the heat shield were kept at the same temperature to prevent heat transfer between them, but the sample was 10 to 40 K cooler than the heat shield. The tantalum foil ring around the sample served as radiation shielding, minimizing radiation heat transfer through the sides of the sample. The tantalum disks behind the sample were needed to cover the hole in the back of the heat shield in order to minimize radiation heat transfer through the back of the sample mount plate. Hence, equation (2) reduces to:

$$Q_{rad} = Q_{rad,f} \quad (3)$$

Thermal conduction losses could occur through the heater leads ( $Q_{c,h}$ ), through the sample thermocouple ( $Q_{c,st}$ ), through the sample mount plate thermocouple ( $Q_{c,pt}$ ), through the prongs used to mount the sample ( $Q_{c,p}$ ), and through air conduction ( $Q_{c,a}$ ):

$$Q_{cond} = Q_{c,h} + Q_{c,st} + Q_{c,pt} + Q_{c,p} + Q_{c,a} \quad (4)$$

All of these conduction losses were made negligible by the experimental design. The heat shield was used as a heat barrier for the sample mount plate so that thermal conduction losses would originate from the heat shield instead of the sample mount plate. The copper heater leads were coiled inside the heat shield to improve thermal contact, therefore minimizing  $Q_{c,h}$ .  $Q_{c,st}$  was made negligible by using a small diameter thermocouple and by wrapping the lead around the heat shield.  $Q_{c,pt}$  was minimized by passing the thermocouple lead through the center of the heat shield.  $Q_{c,p}$  was negligible because the prongs were in good thermal contact with the heat shield (clamped down with set screws) and were in poor thermal contact with the sample (just resting on the surface). The last term,  $Q_{c,a}$ , was negligible because experiments were performed at  $10^{-6}$  torr. In short, equation (3) was reduced to:

$$Q_{cond} = 0 \quad (5)$$

simply by the experimental design.

Combining equations (1), (3), and (5) yields:

$$Q_{el} = Q_{rad,f} - Q_{abs} + mC_p \left( \frac{dT}{dt} \right) \quad (6)$$

Since measurements were made at equilibrium,  $dT/dt = 0$ , and:

$$Q_{el} = Q_{rad,f} - Q_{abs} \quad (7)$$

The power dissipated by the sample mount plate heater,  $Q_{el}$ , could be easily calculated from the equilibrium current (I) and the measured electrical resistance (R):

$$Q_{el} = I^2 R \quad (8)$$

The radiative power emitted ( $Q_{rad,f}$ ) and absorbed ( $Q_{abs}$ ) by the sample are expressed by the Stefan-Boltzmann radiation law:

$$Q_{rad,f} = \epsilon_s \alpha_c \sigma A T_s^4 \quad (9)$$

$$Q_{abs} = \alpha_s \epsilon_c \sigma A T_c^4 \quad (10)$$

where

$\epsilon_s$  total emittance of the sample

$\alpha_s$  total absorptance of the sample

$\epsilon_c$  total emittance of the cavity

$\alpha_c$  total absorptance of the cavity

$\sigma$  Stefan-Boltzmann constant =  $5.6703 \times 10^{-12}$  W-cm<sup>-2</sup>-K<sup>-4</sup>

A sample area (cm<sup>2</sup>)

$T_S$  sample temperature (K)

$T_C$  cavity temperature (K)

By using the above relationships and Kirchoff's law (spectral emittance = spectral absorptance), equation (7) becomes:

$$I^2 R = \epsilon_S \epsilon_C \sigma A (T_S^4 - T_C^4) \quad (11)$$

The cavity was cooled with liquid nitrogen, and the sample temperature was high enough so that  $T_S^4 \gg T_C^4$ . Also, it was shown previously that the cavity was nearly a perfect blackbody, with a total emittance  $\epsilon_C$  very close to unity. Using these facts, the total hemispherical emittance could be calculated directly from:

$$\epsilon_S = \frac{I^2 R}{\sigma A T_S^4} \quad (12)$$

#### UNCERTAINTIES

The total fractional random uncertainty was calculated was from:

$$\left| \frac{\Delta \epsilon_r}{\epsilon} \right| = \sqrt{2 \left( \frac{\Delta I}{I} \right)^2 + \left( \frac{\Delta R}{R} \right)^2 + \left( \frac{\Delta A}{A} \right)^2 + 4 \left( \frac{\Delta T}{T} \right)^2 + \left( \frac{m C_p \left| \frac{dT}{dt} \right|}{I^2 R} \right)^2} \quad (13)$$

The current was measured across a shunt by a millivolt meter and had a probable error of 0.2 percent. Resistance was measured as  $R = V/I$ ; hence,  $\Delta R/R = [(\Delta V/V)^2 + (\Delta I/I)^2]^{1/2}$ , with a probable error in the voltage measurement of 0.06 percent. The sample area was calculated as:

$$A = \frac{\pi d^2}{4} - 4(0.01) \quad (14)$$

where  $d$  was the sample diameter in centimeters. The second term ( $0.04 \text{ cm}^2$ ) was the total area covered by the four wire prongs, with each prong covering  $1 \text{ mm}^2$ ; the estimated uncertainty in this term was  $\pm 0.01 \text{ cm}^2$ . The diameter was measured with digital calipers, having an uncertainty of  $\pm 0.005 \text{ cm}$ . The total uncertainty in the area was therefore:  $\Delta A/A = [2(0.005/d)^2 + (0.01/A)^2]^{1/2}$ . The temperature was measured with a Doric Trendicator 400 A digital meter with an accuracy of  $\pm 1 \text{ K}$ . In order to evaluate the last term of equation (13), the heat capacity of the sample and sample mount plate were needed. The product  $mC_p$  was estimated at room temperature by measuring the power input and time for a 20 K increase in the sample mount plate temperature and was found to be  $4.8 \text{ J-K}^{-1}$ . From this result, it was found that the time required for a 1 K temperature increase with an excess power of 0.01 W was 8 min. Hence, 8 min was taken to be a sufficient equilibrium time for the experiment. The final expression for the total random uncertainty was thus:



$$\left| \frac{\Delta \epsilon_r}{\epsilon} \right| = \sqrt{3(0.002)^2 + (0.0006)^2 + 2\left(\frac{0.005}{d}\right)^2 + \left(\frac{0.01}{A}\right)^2 + 4\left(\frac{1}{T}\right)^2 + \left(\frac{8}{t} \frac{(0.01)}{I^2 R}\right)^2} \quad (15)$$

There were many terms in equations (2) and (3) which were neglected. Most of the conduction terms ( $Q_{c,h}$ ,  $Q_{c,st}$ , and  $Q_{c,p}$ ) were negligible to first order because the objects involved were in good thermal contact with the heat shield, which was at the same temperature as the sample mount plate. The thermocouple lead for the sample mount plate was not in good thermal contact with the heat shield, and  $Q_{c,pt}$  was a possible source of systematic error. The power conducted by the thermocouple lead was estimated to be 0.02 W under the assumption that there was no heat exchanged with the heat shield; thus, the fractional error resulting from the conduction losses was no more than  $(0.02/I^2R)$ . The air conduction term,  $Q_{c,a}$ , was completely negligible under high vacuum. For a pressure of  $5 \times 10^{-6}$  torr, the power lost by air conduction was on the order of  $10^{-4}$  W (ref. 7). Among the radiation terms of equation (2),  $Q_{rad,b}$  was completely negligible to first order because the heat shield was at the same temperature as the sample mount plate and because the opening for the thermocouple and heater leads was very small. There was a significant systematic error from  $Q_{rad,s}$ , however. The sample temperature was often considerably lower than the sample mount plate temperature (up to 40 K). Assuming the foil shielding was at the same temperature as the heat shield, the power absorbed by the sides of the sample was  $\epsilon_e \epsilon_f \sigma A_s (T_{hs}^4 - T_s^4)$ , where  $\epsilon_e$  and  $\epsilon_f$  were the emittances of the edge and the foil (estimated to be 0.3 and 0.1, respectively) and  $A_s$  was the area of the sample edge. The total fractional systematic error was therefore:

$$\begin{aligned} \left| \frac{\Delta \epsilon_s}{\epsilon} \right| &= \frac{Q_{c,st} + Q_{rad,s}}{I^2 R} \\ &= \frac{0.02 + (0.3)(0.1)\sigma A_s (T_{hs}^4 - T_s^4)}{I^2 R} \end{aligned} \quad (16)$$

Combining the results from equations (15) and (16) yielded the total fractional probable error for the experiment:

$$\left| \frac{\Delta \epsilon}{\epsilon} \right| = \sqrt{\left| \frac{\Delta \epsilon_r}{\epsilon} \right|^2 + \left| \frac{\Delta \epsilon_s}{\epsilon} \right|^2} \quad (17)$$

Figure 10 illustrates the dependence of the error on the emittance and temperature of the sample. For high-emitting samples, the fractional error  $|\Delta \epsilon / \epsilon|$  was smallest (0.6 percent) but the absolute error  $\Delta \epsilon$  was largest (0.007). On the other hand, the low-emitting samples had the largest fractional errors (3 percent) and the smallest absolute errors (0.001). The errors were also smaller at higher temperatures. Since the candidate radiator materials to be tested will have high emittances, the CVE measurements will be fairly accurate (< 1 percent) in comparison to Hohraum and open-air emissometer measurements.

## RESULTS AND DISCUSSION

Total emittance measurements were made for eight different samples having a wide range of emittances. For each measurement, there was a difference between the sample temperature and the sample mount plate temperature. Figure 11 shows a plot of the sample temperature versus the sample mount plate temperature for each sample. The high-emitting samples tended to have larger temperature differences than the low-emitting samples because more power had to be conducted through the carbon paint barrier. However, there was no consistent relationship between the emittance and the temperature difference. In order to accurately determine the sample temperature, a thermocouple was directly attached to the back of the sample. Attaching the thermocouple involved considerable time and effort and also involved the possibility of damaging the sample surface. The experiment could be done more quickly but less accurately if a thermocouple was not attached to the sample. The sample temperature would instead be estimated from figure 11 and from the emittance, which could be calculated by iteration. This method would work best for low-emitting materials because the temperature difference would be small.

The total hemispheric emittance results from the CVE and the derived hemispheric-angular Hohlraum reflectometer measurements are plotted in figure 12. For plasma-sprayed alumina (fig. 12(a)), the CVE and Hohlraum results agreed to within 0.01. However, the results from the two instruments did not agree as well for the other materials. The total emittance measured by the CVE was consistently higher than that measured by the Hohlraum reflectometer for the remaining seven samples (figs. 12(b) to (h)). This was to be expected, since the CVE measured total hemispherical emittance, and the Hohlraum measured hemispheric angular emittance. With the exception of the black paint sample (fig. 12(e)), the difference between the results was smaller for the high-emitting samples (figs. 12(b) to (d)) than for the low-emitting samples (figs. 12(f) to (g)). This result is not surprising since the high emittance samples had more diffuse reflectances, therefore their emittance values measured in the Hohlraum reflectometer would be closer to a total hemispherical measurement (ref. 6).

The differences between the results can be attributed in part to errors in the spectral reflectance measurements made by the Hohlraum reflectometer. The uncertainties in the CVE measurements were small (typically less than 1 percent); on the other hand, the uncertainty for the Hohlraum reflectometer was much larger (5 percent) (ref. 9). The Hohlraum reflectometer was especially inaccurate for measuring emittances of polished metals. Emittance values of -0.02 for polished stainless steel (fig. 12(h)) and -0.08 for polished copper (fig. 12(g)) were obtained. These results indicated that the Hohlraum was measuring reflectances greater than unity, which would result from nonuniform temperatures in the Hohlraum's heated cavity. The samples were held in a water-cooled sample holder and were positioned at the top of the cavity, and it was likely that the top of the cavity was cooler than the bottom. If this were the case, the reference beam originating from the top of the cavity would be less intense than the reflected radiation originating mainly from the bottom of the cavity, resulting in a higher measured reflectance and a lower calculated emittance. This would explain the fact that the total emittance measured by the Hohlraum was lower than that measured by the CVE, especially for the samples with low emittance. The only exception was the plasma-sprayed alumina sample (fig. 12(a)), but the spectral emittance of this material is known to decrease significantly at higher temperatures (ref. 10).

One area of agreement for the CVE and Hohlraum total emittance measurements was the temperature dependence of the results. The slopes of the total emittance versus temperature data from the CVE and the Hohlraum agreed for all materials tested, except for a slight difference for sandblasted Nb (1 percent Zr) (fig. 12 (d)). All materials tested except for plasma-sprayed alumina (fig. 12(a)) showed an increase in total emittance with temperature.

Total emittance as a function of temperature was also obtained for plasma-sprayed alumina and high temperature black paint by normalizing the spectral emittance measured at elevated temperature (873 K) in air using the emissometer attachment. These data are shown in figure 13, along with emittance measurements from the CVE and the Hohlraum. For the plasma-sprayed alumina, there was close agreement between the CVE and emissometer. The emittance values differed by no more than 0.02. Oxidation was a problem whenever elevated temperature measurements were made in air (ref. 4). One would not expect this problem for the plasma-sprayed alumina, which was already oxidized. To eliminate the oxidation effect for the black paint sample, the emissometer measurements were done before the CVE measurements in order to insure that the sample was fully oxidized in both cases. The surface texture for the plasmasprayed alumina was very rough in comparison to the black paint, and the alumina was more likely a diffuse reflector than the black paint. The black paint sample would therefore exhibit directional effects to a greater extent, and this could explain the differences between the CVE and emissometer measurements. Also, temperature effects were confirmed to be significant. Figures 13(a) and (b) compare total emittance versus temperature measured by the room temperature Hohlraum reflectometer to the other elevated temperature techniques. There were large differences in the Hohlraum and emissometer results for alumina below 700 K and for the black paint at all temperatures.

#### CONCLUDING REMARKS

The CVE was successful in measuring the total hemispherical emittance of candidate space radiator materials at elevated temperatures. The CVE has several advantages over the Hohlraum reflectometer and emissometer attachments. The probable error of the CVE (typically less than 1 percent) is smaller than that of the Hohlraum or the emissometer ( $\pm 5$  percent). Since measurements are performed under vacuum, samples measured in the CVE do not have problems with oxidation or other chemical processes which might occur in the open-air emissometer. CVE measurements are made at elevated temperature, while Hohlraum measurements are calculated from room temperature data. Directional effects also play a significant part in the Hohlraum and emissometer measurements, which measure hemispheric-angular and normal spectral emittance, respectively. In short, the CVE accurately measures total hemispherical emittance in vacuum at elevated temperatures, which is the desired engineering value for space radiator design; the Hohlraum and the emissometer do not.

Nonetheless, there is an important advantage for the Hohlraum reflectometer. A Hohlraum measurement requires less than an hour, while a CVE measurement takes much longer because of the time required to attach the thermocouple to the sample, pump down the system, and bring the sample temperature to equilibrium. Hohlraum measurements are also fairly accurate for diffusely reflecting samples. Hence, the Hohlraum reflectometer is ideal for screening candidate radiator materials. The materials with high emittances measured in

the Hohlraum could then be measured in the CVE to obtain more reliable measurements.

#### REFERENCES

1. S.K. Rutledge, B.A. Banks, M.J. Mirtich, R. Lebed, J. Brady, D. Hotes, and M. Kussmaul, "High Temperature Radiator Materials for Applications in the Low Earth Orbital Environment," NASA TM-100190, 1987.
2. M.J. Mirtich and M.T. Kussmaul, "Enhanced Thermal Emittance of Space Radiators by Ion-Discharge Chamber Texturing," NASA TM-100137, 1987.
3. B.A. Banks, S.K. Rutledge, M.J. Mirtich, T. Behrend, D. Hotes, M. Kussmaul, J. Barry, C. Stidham, T. Stueber, and F. DiFilippo, "Arc-Textured Metal Surfaces for High Thermal Emittance Space Radiators," NASA TM-100894, 1988.
4. M. Mirtich, F. DiFilippo, J. Barry, and M. Kussmaul, "The Emittance of Space Radiator Materials Measured at Elevated Temperatures," NASA TM-101948, 1988.
5. J.C. Richmond, ed., Measurement of Thermal Radiation Properties of Solids, NASA SP-31, (National Aeronautics and Space Administration, Washington, D.C., 1963).
6. R. Siegel and J.R. Howell, in Thermal Radiation Heat Transfer, Second Edition, (Hemisphere Publishing Corp., Washington, D.C., 1981) Chapter 5.
7. G.T. O'Connor, "Thermal Radiation from Hot Surfaces Measured by Optical and Calorimetric Methods," M.S. Thesis, University of Arizona, 1982.
8. W.L. Wolfe and G.J. Zissis, eds., The Infrared Handbook, (Office of Naval Research, Dept. of the Navy, Washington, D.C., 1978) pp. 2-2 to 2-4.
9. "Infrared Reflectivity Attachments," Manual from the Perkin-Elmer Corp., Norwalk, CT, p. 3.
10. C.H. Liebert, "Spectral Emittance of Aluminum Oxide and Zinc Oxide on the Opaque Substrates," NASA TN D-3115, 1965.

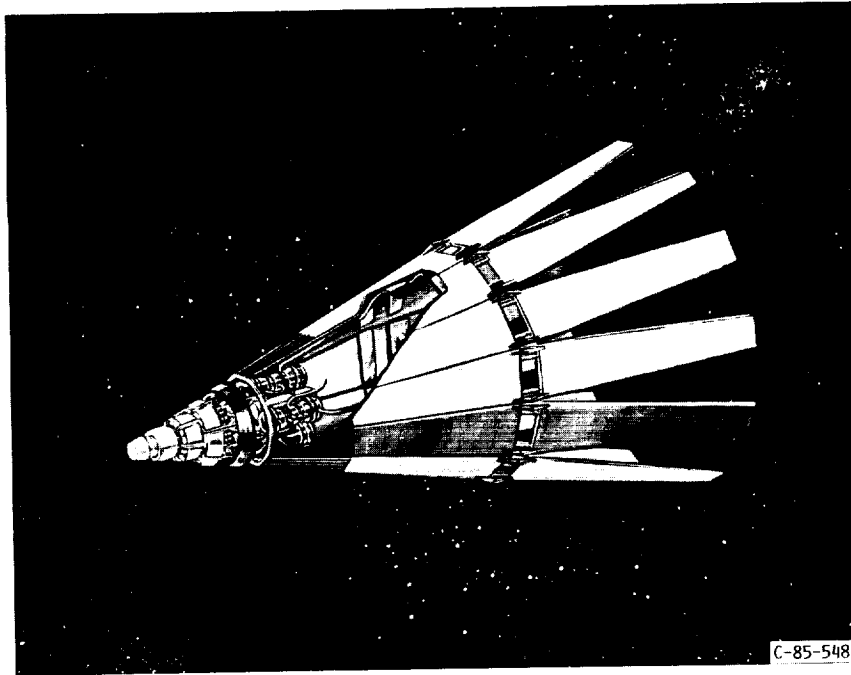


FIGURE 1. - SP100 SPACE NUCLEAR POWER SYSTEM (RADIATOR PANELS COMPRISE THE EXTERIOR OF THE SYSTEM).

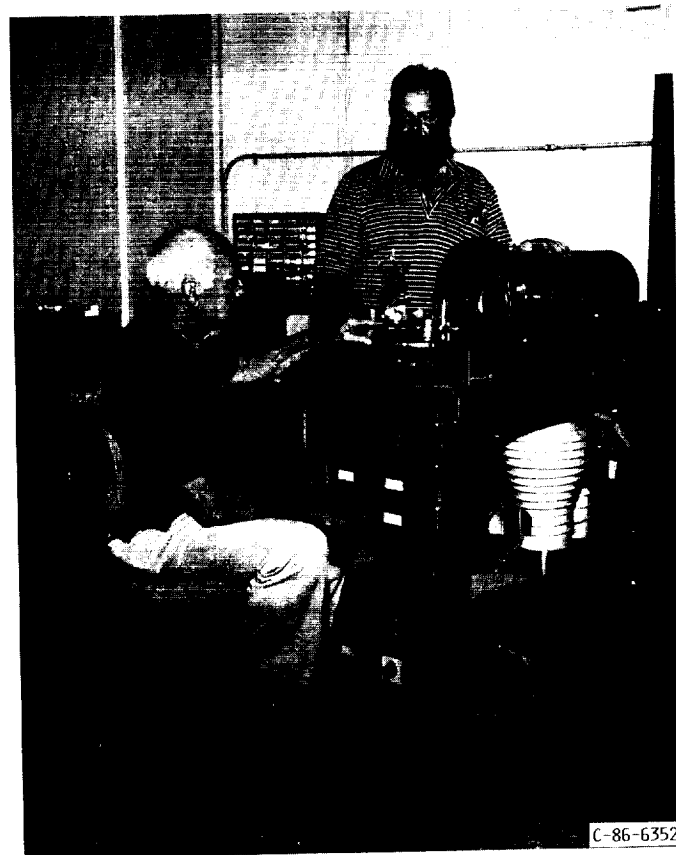


FIGURE 2. - CVF VACUUM CHAMBER AND PUMP SYSTEM.



FIGURE 3. - CVL SAMPLE HOLDER.

C-88-6358

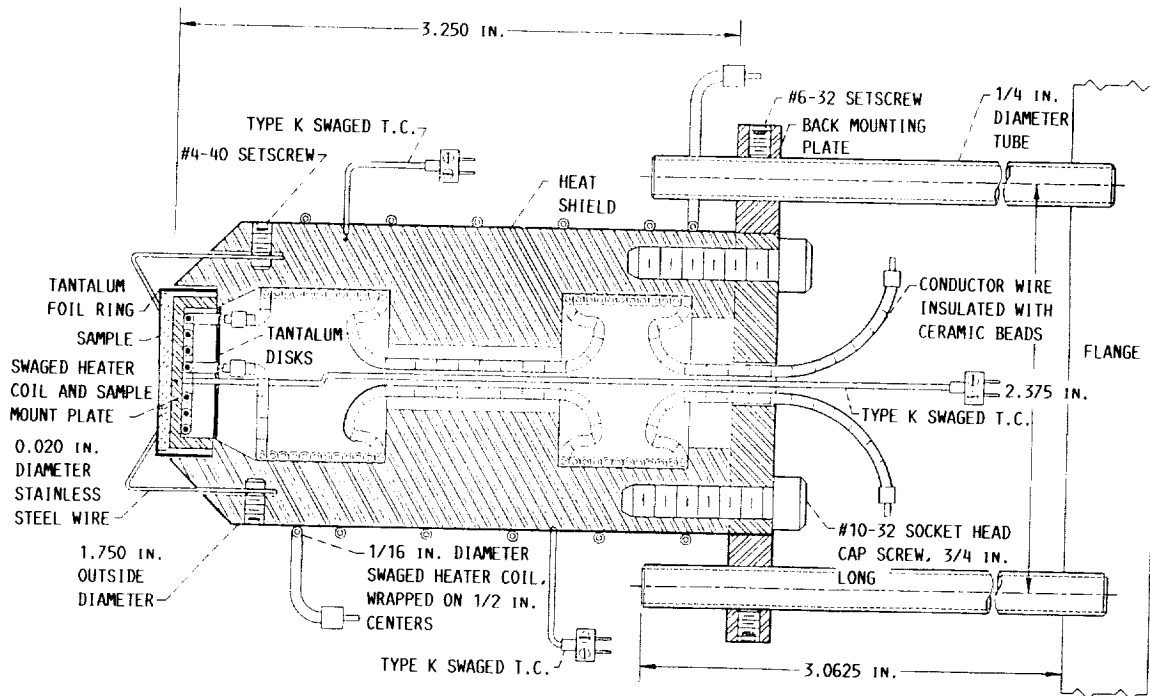


FIGURE 4. - CUTAWAY DRAWING OF THE CVE HEATER/HOLDER.

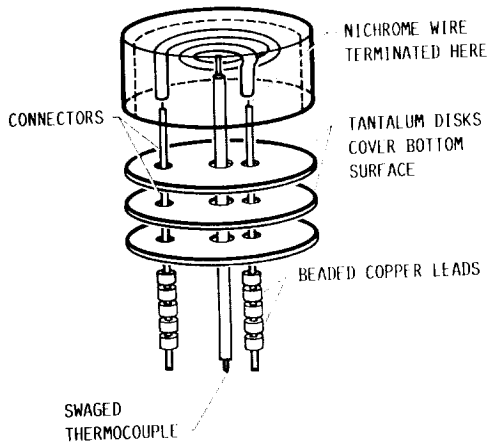


FIGURE 5. - SAMPLE MOUNT PLATE.

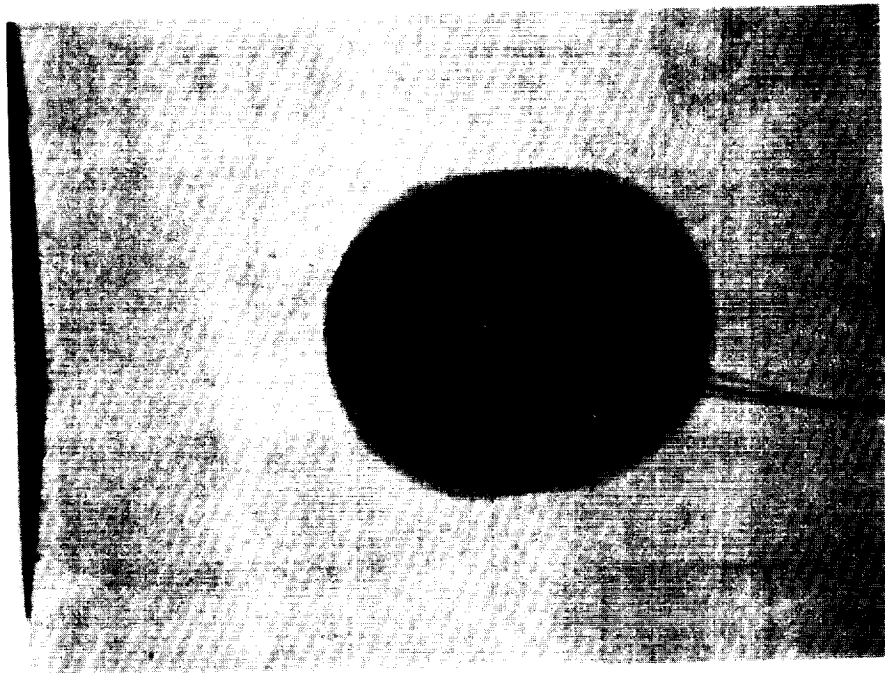


FIGURE 6. - PHOTO OF THERMOCOUPLE SAMPLE (BACK SURFACE).

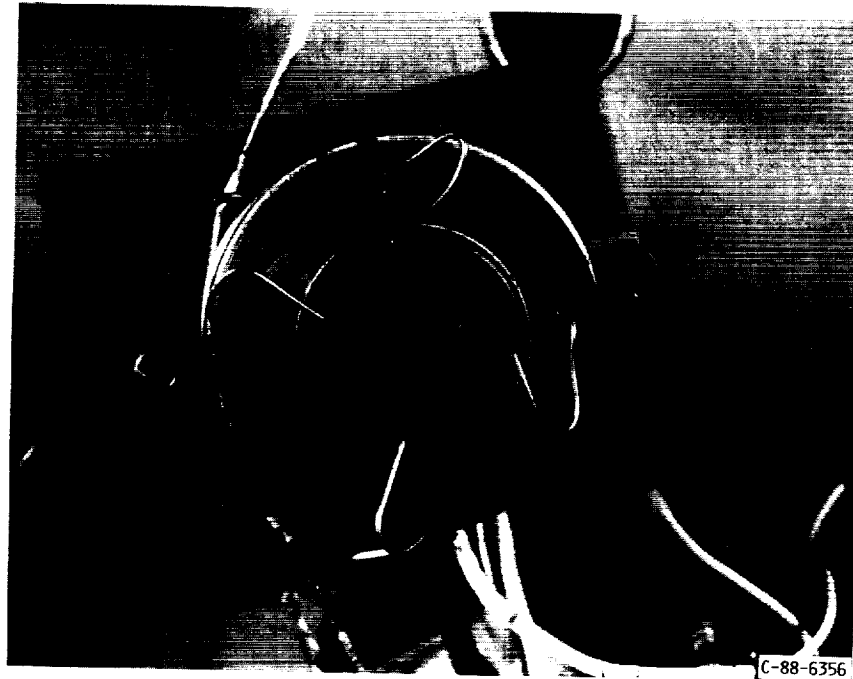


FIGURE 7. MOUNTED SAMPLE.

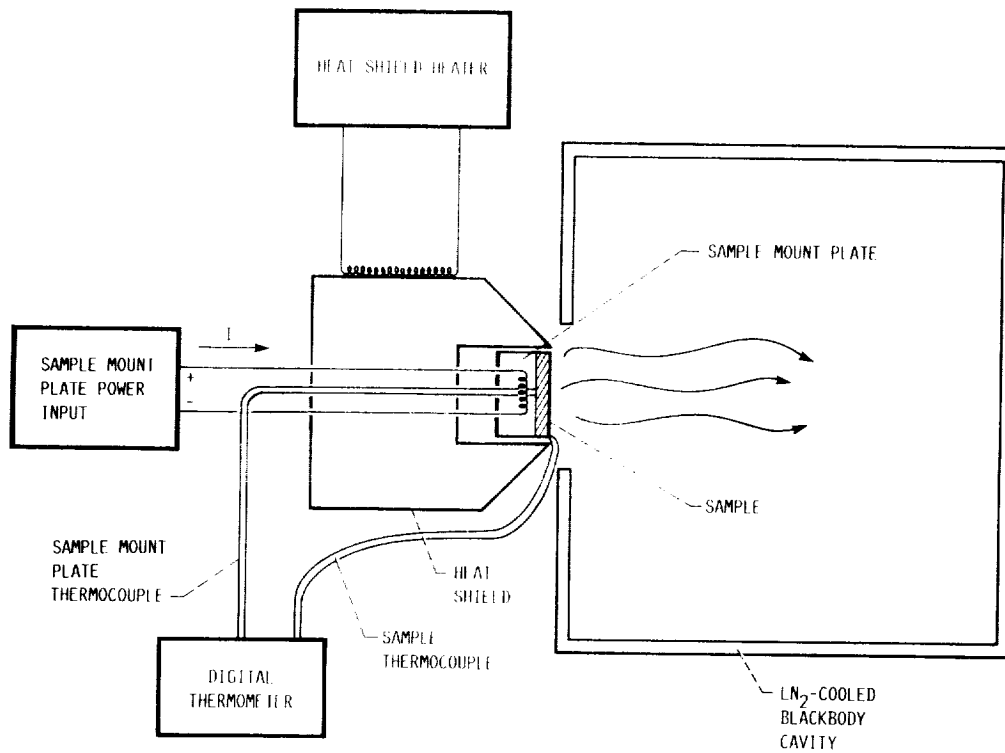


FIGURE 8. SCHEMATIC OF THE EXPERIMENT.



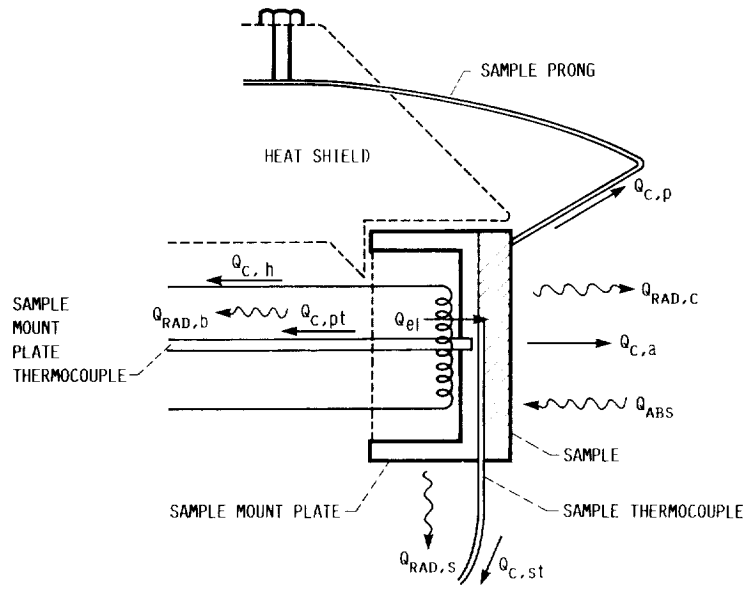
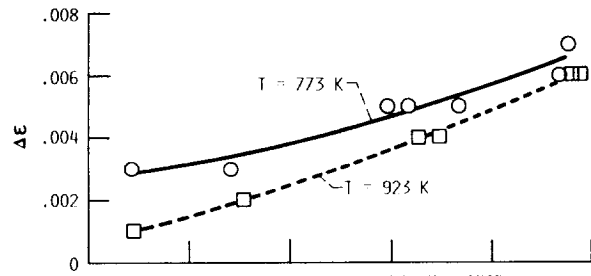
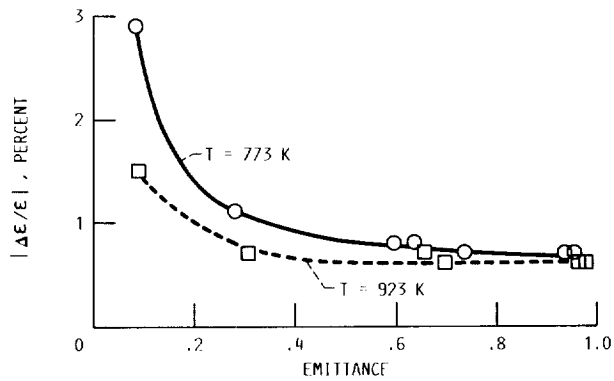


FIGURE 9. - HEAT TRANSFER SCHEMATIC.



(a) ABSOLUTE ERROR VERSUS EMITTANCE.



(b) FRACTIONAL ERROR VERSUS EMITTANCE.

FIGURE 10. - PROBABLE ERROR AS A FUNCTION OF EMITTANCE AND TEMPERATURE.

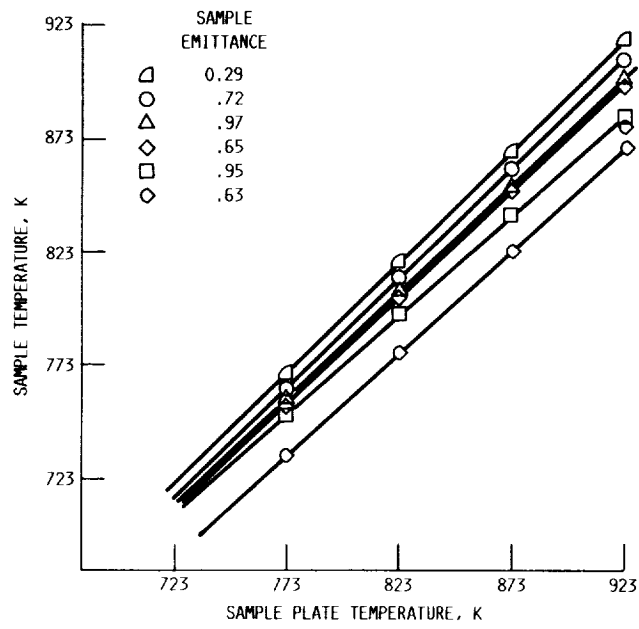


FIGURE 11.- SAMPLE TEMPERATURE AS A FUNCTION OF SAMPLE PLATE TEMPERATURE FOR SAMPLES OF VARIOUS EMITTANCES.

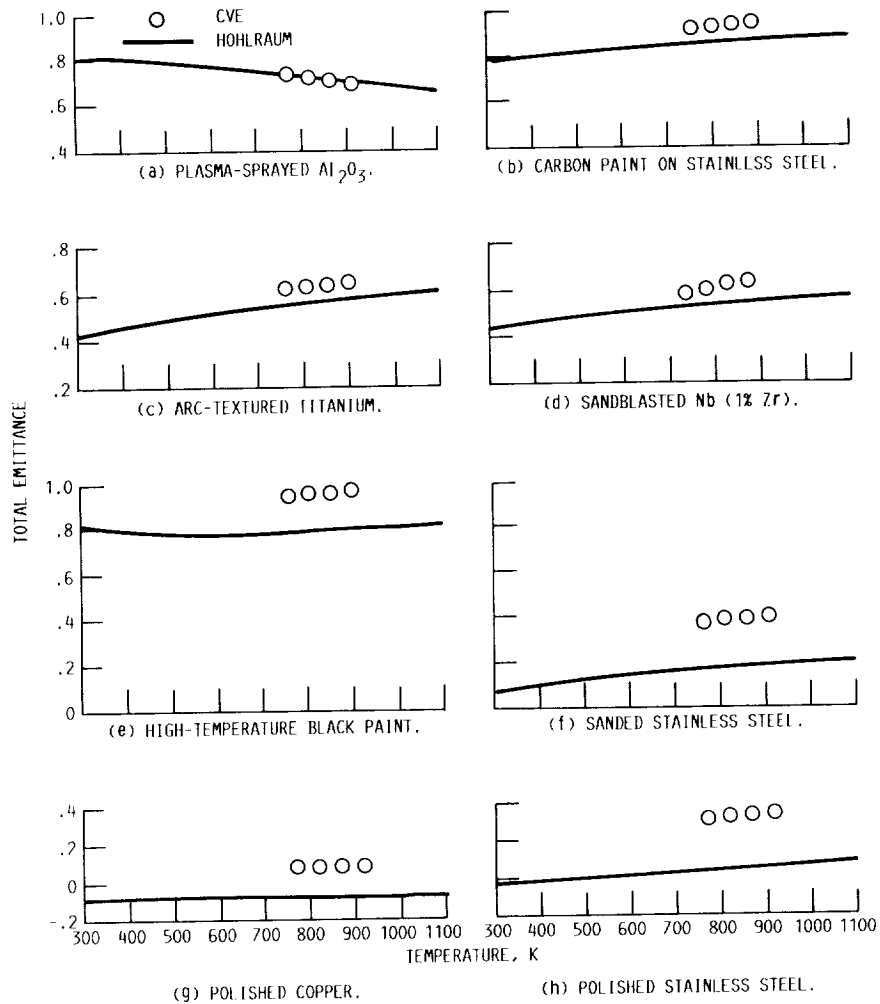


FIGURE 12. - CVE TOTAL HEMISPHERIC EMITTANCE AND HOHLRAUM HEMISPHERIC-ANGULAR EMITTANCE MEASUREMENTS.

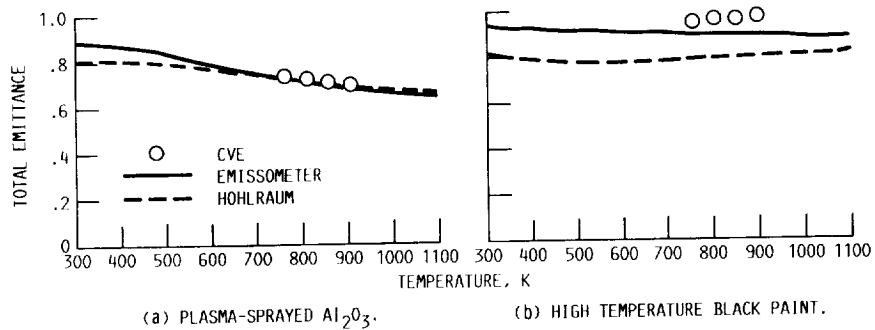


FIGURE 13. - TOTAL EMITTANCE MEASURED WITH THE EMISSOMETER AND THE CVE.

# Report Documentation Page

1. Report No. NASA TM-102322		2. Government Accession No.		3. Recipient's Catalog No.	
4. Title and Subtitle Total Hemispherical Emittance Measured at High Temperatures by the Calorimetric Method				5. Report Date	
				6. Performing Organization Code	
7. Author(s) Frank DiFilippo, Michael J. Mirtich, Bruce A. Banks, Curtis Stidham, and Michael Kussmaul				8. Performing Organization Report No. E-4704	
				10. Work Unit No. 586-01-11	
9. Performing Organization Name and Address National Aeronautics and Space Administration Lewis Research Center Cleveland, Ohio 44135-3191				11. Contract or Grant No.	
				13. Type of Report and Period Covered Technical Memorandum	
12. Sponsoring Agency Name and Address National Aeronautics and Space Administration Washington, D.C. 20546-0001				14. Sponsoring Agency Code	
				15. Supplementary Notes Prepared for the 16th International Conference on Metallurgical Coatings sponsored by the American Vacuum Society, San Diego, California, April 17-21, 1989.	
16. Abstract A calorimetric vacuum emissometer (CVE) capable of measuring total hemispherical emittance of surfaces at elevated temperatures was designed, built, and tested. Several materials with a wide range of emittances were measured in the CVE between 773-923 K. These results were compared to values calculated from spectral emittance curves measured in a room temperature Hohlraum reflectometer and in an open-air elevated temperature emissometer. The results differed by as much as 0.2 for some materials but were in closer agreement for the more highly-emitting, diffuse-reflecting samples. The differences were attributed to temperature, atmospheric, and directional effects, and errors in the Hohlraum and emissometer measurements ( $\pm 5\%$ ). The probable error of the CVE measurements was typically less than 1%.					
17. Key Words (Suggested by Author(s)) Emittance Calorimetry Emissivity			18. Distribution Statement Unclassified - Unlimited Subject Category 31		
19. Security Classif. (of this report) Unclassified		20. Security Classif. (of this page) Unclassified		21. No of pages 18	22. Price* A03



National Aeronautics and  
Space Administration

**Lewis Research Center**  
Cleveland, Ohio 44135

**Official Business**  
Penalty for Private Use \$300

**FOURTH CLASS MAIL**

ADDRESS CORRECTION REQUESTED



Postage and Fees Paid  
National Aeronautics and  
Space Administration  
NASA 451

**NASA**

---

DAA JUL 08 1989 RE

To be initiated by the responsible NASA Project Officer, Technical Monitor, or other appropriate NASA official for all presentations, reports, papers, and proceedings that contain scientific and technical information. Explanations are on the back of this form and are presented in greater detail in NHB 2200.2, "NASA Scientific and Technical Information Handbook."

Original  
 Modified

(Facility Use Only)  
Control No. \_\_\_\_\_  
Date \_\_\_\_\_

I. DOCUMENT/PROJECT IDENTIFICATION (Information contained on report documentation page should not be repeated except title, date and contract number)  
Title: Total Hemispherical Emittance Measured at High Temperature by the Calorimetric Method  
Author(s): M. Mirtich, F. DiFilippo, B. Banks, C. Stidham, M. Kussmaul  
Originating NASA Organization: Lewis Research Center  
Performing Organization (if different) \_\_\_\_\_  
Contract/Grant/Interagency/Project Number(s): 586-01-11  
TM102322 Document Date: \_\_\_\_\_  
Document Number(s) \_\_\_\_\_  
(For presentations or externally-published documents, enter appropriate information on the intended publication such as name, place, and date of conference, periodical or journal title, or book title and publisher: 16th International Conf. on Metallurgical Coatings, San Diego, CA.  
These documents must be routed to NASA Headquarters, International Affairs Division for approval. (See Section VII) April 17-21, 1989

II. AVAILABILITY CATEGORY  
Check the appropriate category(ies):  
Security Classification:  Secret  Secret RD  Confidential  Confidential RD  Unclassified  
Export Controlled Document - Documents marked in this block must be routed to NASA Headquarters International Affairs Division for approval.  
 ITAR  EAR  
NASA Restricted Distribution Document  
 FEDD  Limited Distribution  Special Conditions-See Section III  
Document disclosing an invention  
 Documents marked in this block must be withheld from release until six months have elapsed after submission of this form, unless a different release date is established by the appropriate counsel. (See Section IX).  
Publicly Available Document  
 Publicly available documents must be unclassified and may not be export-controlled or restricted distribution documents.  
 Copyrighted  Not copyrighted

IN-51  
232683  
198

III. SPECIAL CONDITIONS  
Check one or more of the applicable boxes in each of (a) and (b) as the basis for special restricted distribution if the "Special Conditions" box under NASA Restricted Distribution Document in Section II is checked. Guidelines are provided on reverse side of form.  
a. This document contains:  
 Foreign government information  Commercial product test or evaluation results  Preliminary information  Information subject to special contract provision  
 Other - Specify \_\_\_\_\_  
b. Check one of the following limitations as appropriate:  
 U.S. Government agencies and U.S. Government agency contractors only  NASA contractors and U.S. Government agencies only  U.S. Government agencies only  
 NASA personnel and NASA contractors only  NASA personnel only  Available only with approval of issuing office: \_\_\_\_\_

IV. BLANKET RELEASE (OPTIONAL)  
All documents issued under the following contract/grant/project number \_\_\_\_\_ may be processed as checked in Sections II and III.  
The blanket release authorization granted \_\_\_\_\_ Date \_\_\_\_\_ is:  
 Rescinded - Future documents must have individual availability authorizations.  Modified - Limitations for all documents processed in the STI system under the blanket release should be changed to conform to blocks as checked in Section II.

V. PROJECT OFFICER/TECHNICAL MONITOR  
Bruce Banks 5400 Bruce Banks/cib 12-13-88  
Typed Name of Project Officer/Technical Monitor Office Code Signature Date

VI. PROGRAM OFFICE REVIEW  Approved  Not Approved  
R.E. ROSE RE R.E. Rose 11/9/89  
Typed Name of Program Office Representative Program Office and Code Signature Date

INTERNATIONAL AFFAIRS DIVISION REVIEW  
 Open, domestic conference presentation approved.  Export controlled limitation is not applicable.  
 Foreign publication/presentation approved.  The following Export controlled limitation (ITAR/EAR) is assigned to this document: \_\_\_\_\_  
 Export controlled limitation is approved.  
D.A. VIC JAN 26 1989  
International Affairs Div. Representative Title Date

PIRATION OF REVIEW TIME  
Document is being released in accordance with the availability category and limitation checked in Section II since no objection was received from the Program in 20 days of submission, as specified by NHB 2200.2, and approval by the International Affairs Division is not required.  
Office Code \_\_\_\_\_ Date \_\_\_\_\_  
Release procedure cannot be used with documents designated as Export Controlled Documents, conference presentations or foreign publications.

INTS DISCLOSING AN INVENTION  
Document may be released on \_\_\_\_\_ Date \_\_\_\_\_  
Installation Patent or Intellectual Property Counsel \_\_\_\_\_  
was processed on \_\_\_\_\_ Date \_\_\_\_\_  
in accordance with Sections II and III as applicable. NASA STI Facility \_\_\_\_\_ Date \_\_\_\_\_

ould be forwarded to the NASA Scientific and Technical  
P.O. Box 8757, B.W.I. Airport, Maryland 21240, with

ducible copy of document enclosed  
nt Documentation Page enclosed. The issuing or sponsoring NASA installation should provide a copy of the document, when complete.  
ntific and Technical Information Facility at the above listed address.

VII. EX
VIII. EX The docu Office with Name & Titl Note: This r
IX. DOCUME a. This docum b. The document
X. DISPOSITION Completed forms sh Information Facility, either (check box): <input type="checkbox"/> Printed or repro <input type="checkbox"/> Abstract or Repro to the NASA Sci